# Journal of Materials Chemistry C

Accepted Manuscript


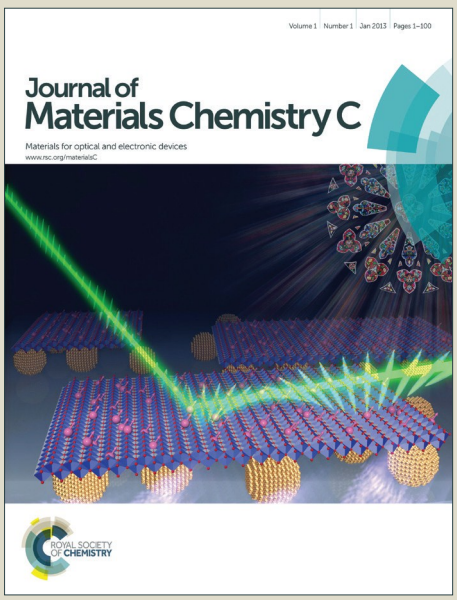





ROYAL SOCIETY OF CHEMISTRY

www.rsc.org/materialsC

Cite this: DOI: 10.1039/c0xx00000x

www.rsc.org/xxxxxx

ARTICLE TYPE

# Controllable Fabrication of Nickel Nanoparticle Chains Based on Electrochemical Corrosion

**Shao Hui Xu, Guang Tao Fei*, Hao Miao Ouyang, Yao Zhang, Peng Cheng Huo and Li De Zhang**

***Received (in XXX, XXX) XthXXXXXXXXX 20XX, Accepted Xth XXXXXXXXX 20XX***

**DOI: 10.1039/b000000x**

Magnetic nanoparticle (NP) chain has attracted great concern due to its potential applications in magnetic recording, electron nano-device, micro-mechanical sensor, drug delivery and so on. Here, we demonstrate the controllable preparation of magnetic Ni NP chains by using electrochemical corrosion methods. Ni/Cu multi-segmented nanowires (NW) are firstly prepared by alternately depositing Ni and Cu into the pores of anodic aluminum oxide (AAO) template, then highly uniform Ni NP chains are obtained by immersing Ni/Cu NWs/AAO composite membrane in 15wt% NaOH solution for about 50min.The reaction mechanism is proposed based on electrochemical corrosion, in which Cu serviced as the anode are corroded and Ni serviced as the cathode are retained in NaOH electrolyte solution. Particle size and separation of the Ni NP chains can be easily adjusted and the smallest particle size and particle spacing reach to 6nm and 15nm, respectively. This strategy developed herein can be expected as a general route for controllable fabrication of metallic NP chains.

## 1 Introduction

Nanomaterials with advanced construction can be used as the unit to build the device with special properties.[1,2] It was found that novel collective properties will emerge in the ordered array of nanoparticles (NPs) that significantly different from the single one.[3] Metallic NP chains as one kind of an ordered nanostructure have recently attracted wide attention for their novel properties in optics,[4-7] electronics,[8,9] photonic,[10,11] magnetics[12-14] and sense,[15,16] etc. For example, noble metallic NP chain was thought to be a promising plasmonic waveguide structure and be expected to apply in nano-optical waveguide devices.[4-7] Besides, because of the intriguing magnetic properties, magnetic NP chains have attracted great concern for their potential applications in magnetic recording, electron nano-device, micro-mechanical sensor, drug delivery and so on.[14] Previous studies have illustrated that in Ni NP chains, there will emerge several interesting effects, including the ferromagnetic[17] or antiferromagnetic[18] order and significant enhancement of coercivity.[17] Besides, ultra-high density data storage,[19] with the storage densities of over 1 Tbit inch$^{-2}$, was also investigated in magnetic NPs chain when the magnetic particles arranged in ordered arrays with individual domain size below 50nm.[20]

It is reported that the performance of the NP chains are strongly related to the particle size, shape and separation. So far, various available assembly routes such as electron beam lithography, scanning-probe manipulation,[5-7, 21] self-assemble,[22-25] exploitation of the Rayleigh instability,[26-29] wet-chemistry etching,[30-32] and solid-state reactions at high temperature[33,34] have been used to prepare metal NP chains. However, these avenues were mainly used to prepare noble metallic NP chains, such as Au,[5,6,27] Pt,[33,34] Cu.[26,28,29] For magnetic NP chains, the general preparation route is the self-assemble method. By using the soft-templates or the applied magnetic field, Ni NP chain structures can be achieved.[35,36] Recently, magnetic Co NP chains wrapped by the scrolled niobate nanosheets (NSs) were prepared by firstly assembling Co NP on the surface of niobate NSs and then scrolling niobate NSs around magnetically aligned Co NP chains.[37] However, the separation in the NP chains prepared by self-assembly method is found too hard to control, which significantly retard their applications. To extend the applications of the NP chains, it is highly desirable to develop a new and controllable avenue to prepare the magnetic NP chains structures.

Herein, we report a controllable route to fabricate Ni NP chains. Highly uniform Ni NP chain structures consisting of Ni NPs linked with thin CuO film, were prepared by alternate electrodeposition of Ni/Cu multi-segmented NWs into the pores of anodic aluminum oxide (AAO) template and subsequently corrosion in alkali solution. The reaction mechanism was discussed in detail, in which the neighboring Ni segments and Cu segments would constitute the primary batteries in NaOH electrolyte, and the Cu anode is electrochemical corroded and the Ni cathode is reserved. The reaction residue CuO thin film between Ni NPs just plays a role in connecting. Besides, the particle size and separation of the NPs can be adjusted successfully. Our findings inspire a universal and convenience way for the NP chains structures preparation.

## 2 Experimental section

Fabrication of Ni NP chains is schematically illustrated in Fig. 1. Firstly, Ni/Cu multi-segmented NWs were electrodeposited into the pores of nanoporous AAO template. After electrodeposition,

the Ni/Cu NWs/AAO composite membrane was immersed in 15wt% NaOH solution for about 50min, then washed with distilled water and absolute ethanol, and dispersed on silicon slice by ultrasonication.

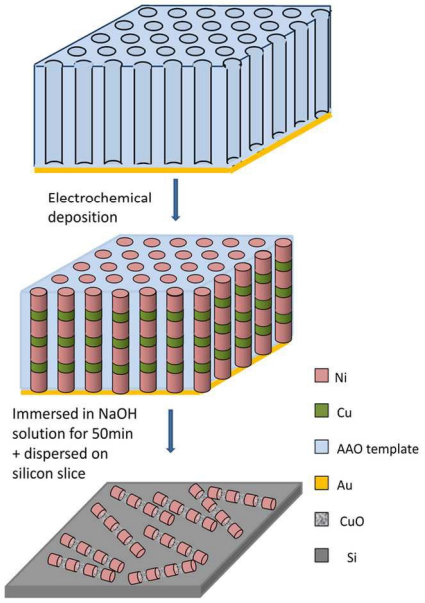


**Fig. 1** The schematic diagram for preparation of Ni NP chains.

### 2.1 Preparation of the AAO template

The AAO templates were prepared via a two-step anodization process.[38] After the anodization, the back aluminum was removed in a saturated$CuCl_2$ solution, then the barrier was dissolved in 5 wt% phosphoric acid solution at 40 °C for 25 min and the double-opened AAO templates with pore size about 50 nm were obtained. After then, an Au layer with thickness of about 200 nm was sputtered onto one side of the double-opened AAO template as the working electrode.

### 2.2 Electrodeposition of Ni/Cu nanowires

Table 1. The detailed deposition parameters of Ni/Cu NWs.

| Samples | Composition | Current(mA) | Deposition time (s) | Cleaning time (s) |
|---|---|---|---|---|
| 1 | Ni/Cu | 2.0/0.8 | 10/15 | 60/60 |
| 2 | Ni/Cu | 1.5/0.8 | 5/10 | 60/60 |
| 3 | Ni/Cu | 1.5/0.8 | 30/15 | 60/60 |
| 4 | Ni/Cu | 2.5/0.8 | 60/30 | 60/60 |

Ni/Cu multi-segmented nanowires were fabricated with the alternate electrodeposition method.[39] All the processes can be described briefly as follows: two elements of Ni and Cu were electrodeposited alternately into the AAO template in different electrolytic cells, and all the processes were controlled by a home-made programmed device. The electrolyte used for deposition of Ni consisted of 0.38 M $NiSO_4{\cdot}6H_2O$, 0.12 M $NiCl_2{\cdot}6H_2O$ and 0.5 M $H_3BO_3$, and the pH value was adjusted to about 2.5 with 1 M $H_2SO_4$; the electrolyte used for Cu depositing contained 0.2 M $CuSO_4{\cdot}5H_2O$ and 0.5 M $H_3BO_3$ with pH value of about 2.5 adjusted by 1 M $H_2SO_4$. The detailed deposition parameters such as deposition potential, deposition current and deposition time of each element were listed in Table 1.

### 2.3 Fabrication of Ni NP chains

After electrodeposition, Ni/Cu NWs/AAO composite membrane was immersed in 15wt% NaOH solution and corroded for about 50min. During the corrosion process, the AAO template was firstly removed by the NaOH solution, and then Ni/Cu NWs released from the AAO would fully contact with the NaOH solution, resulting in the corrosion of periodic composition of Cu in the Ni/Cu NWs. Then the specimen was rinsed with distilled water and absolute ethanol for several times to clear the residues, finally the Ni NP chains linked by CuO film was obtained.

### 2.4 Characterization

The morphology of nanostructure was characterized by a field emission scanning electron microscopy (FE-SEM, FEI Sirion 200); the crystal structure and chemical component were studied by transmission electron microscope (TEM, JEOL-2010), high resolution TEM (HRTEM), and energy dispersive X-ray spectroscopy (EDS) elements line scanning attached to the TEM. For the observation of Ni/Cu multi-segmented NWs arrays, the specimen was released from the AAO with 5 wt% NaOH solution for about 15 min to remove AAO template and then directly attached on the sample platform for the FE-SEM observation. For the observation of dispersed NP chains, the specimen was ultrasonically dispersed in the ethanol for 2-3 minutes, and then several droplets of ethanol dispersed with samples were dropped on a piece of silicon wafer and dried for FE-SEM observation, and several droplets of ethanol dispersed with samples were put on a copper grid covered with carbon films and dried for TEM analysis.

## 3 Results and discussion

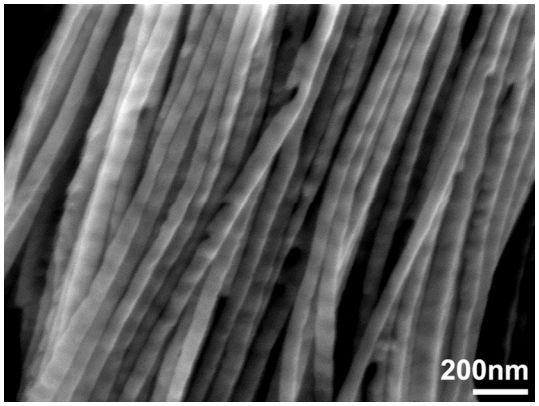


**Fig.2** The FE-SEM image of Ni/Cu multi-segmented NWs arrays in sample 1.

### 3.1 Morphology comparison before and after corroding

We firstly observed the morphology of Ni/Cu multi-segmented nanowire arrays before corrosion. Fig. 2 shows the FE-SEM images of Ni/Cu multi-segmented NWs arrays of sample 1, in which these NWs have the uniform diameter and smooth surface. The alternating contrast changes in NWs demonstrate the periodic distribution of two components. Fig. 3a is the FE-SEM image of sample 1 after corroding for about 50 min, periodic dark strips appear along the longitudinal axis of each wire, indicating the component was periodically corroded and the NP chains structure formed. Fig. 3b displays the TEM image of the NP chain,

from which we can see that the nanostructure exhibit periodic heterogeneous contrast obviously. From the magnified inset in fig. 3b, we can estimate the particle size is about 35 nm and the separation is about 20 nm. In order to determine the precise component distribution of the NP chain, the EDS elements line scanning analysis was carried out and shown in the fig.4. It can be seen that Ni X-ray signals display periodic modulation and Cu X-ray signal is quiet small and nearly approach to zero. Therefore, the component of the NP chain can be regarded as mainly composed of Ni with periodic distribution and the Cu is almost removed.

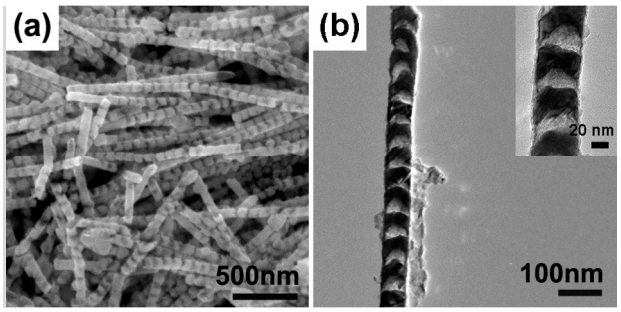


**Fig.3** (a) The FE-SEM image of the NP chains obtained after corroding sample 1 by 15wt% NaOH solution for about 50min and dispersed on silicon. (b) The TEM image of the NP chain, and the inset is magnified image.

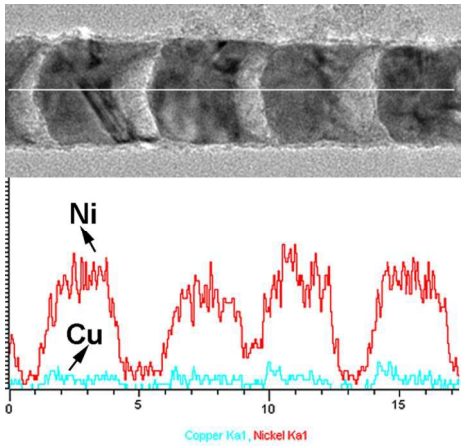


**Fig.4** The TEM image of a single NP chain and the corresponding EDS elements line scanning image.

### 3.2 Particle size and distance regulation

Particle size and separation of the NP chains can be easily adjusted by controlling the deposition time of Cu and Ni. When shorten the deposition time of each element to Ni5s/Cu10s, that is, the respective deposition times of Ni and Cu are 5 s and 10 s, sample 2 with shorter periodic length was obtained, which can be clearly seen from the fig. 5. Fig. 5a and 5b show the TEM images with different magnification of sample 2 after corroding by 15 wt% NaOH solution for about 50 min. It can be seen that the NP chains have uniform structures and maintain good periodicity, demonstrating Ni has a good retention during the Cu removal process. From fig. 5b we can estimate the segment length of Ni is about 6 nm and the separation is about 15 nm, respectively. Prolonging the deposition time of each element, Ni30s/Cu15s (sample 3) and Ni60s/Cu30s (sample 4) with longer segment lengths were obtained. Fig. 5c shows the FE-SEM image of sample 3 after corroding under the same condition, and fig. 5d gives the corresponding TEM image. It can be seen that the length of Ni segment is about 50 nm, and the separation between Ni segments is of about 25 nm. By the way, these one dimensional NP chains display bending in some degree. Fig. 5e and 5f correspond to the FE-SEM images with different magnification for sample 4 after corroding, which show a longer Ni segment of about 110 nm and a larger separation of about 50 nm. From the morphology images of all samples, we can find that the obtained NP chains possess a stable structure and can mainly retain the morphology of NWs even with some degree of bending. The above results indicate that the sizes of Ni segment and the separation can be adjusted easily. The minimum particle size of Ni chains can reach to 6 nm and the minimum separation between Ni particles can reach to 15 nm in our experiment.

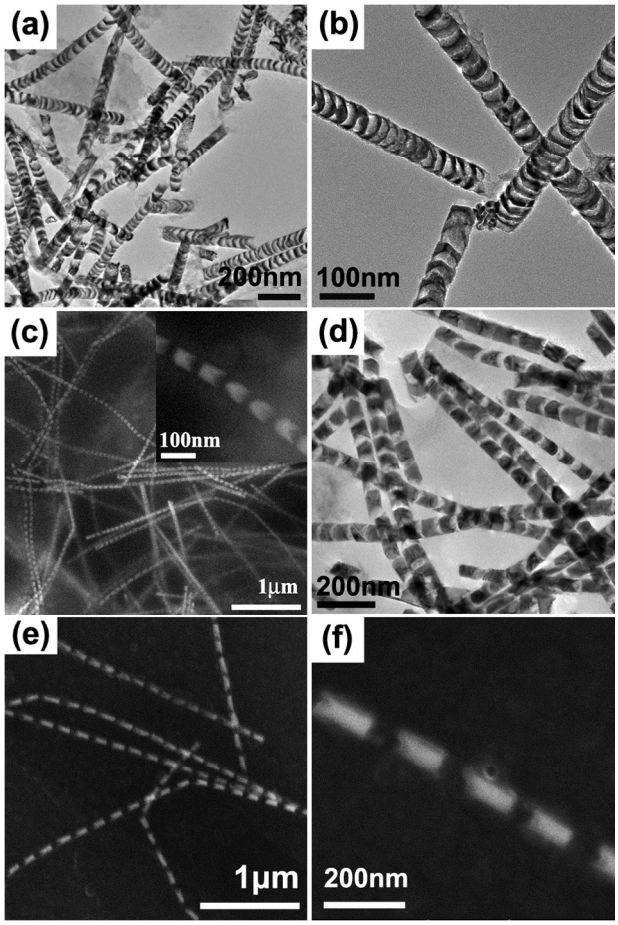


**Fig.5** The TEM images of the Ni NP chains obtained by corroding sample 2 using 15wt% NaOH solution for about 50min, at lower (a) and higher (b) magnification. The SEM image (c) and TEM image (d) of the NP chains obtained by corroding sample 3 using 15wt% NaOH solution for about 50min. (e) and (f) The SEM image of the NP chains with different magnification obtained when sample 4 etched by 15wt% NaOH solution for about 50min.

### 3.3 Detailed composition analysis

Strikingly, the Ni NPs were not dispersed after the Cu segments corroded, and the NWs structures are still retained. To better understand the connection between the neighboring Ni segments, HRTEM was adopted to reveal the interface of the Ni NP chains.

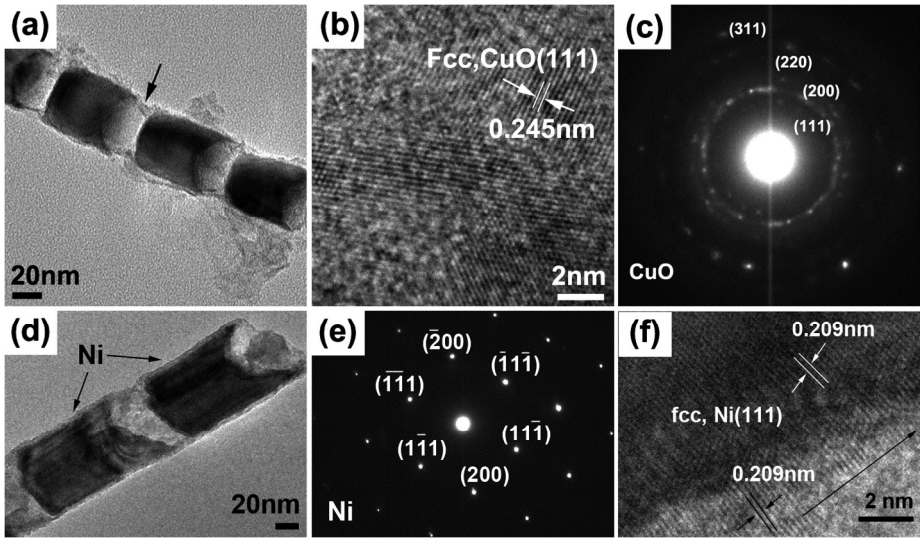


**Fig.6** (a) The TEM image of singe Ni NP chain. (b) and (c) The HR-TEM image and SAED pattern for the part labeled in (a) with arrow. The high magnification of TEM image of Ni segments (d) and the corresponding SAED pattern (e) and HR-TEM image (f).

Fig. 6a shows the TEM image of Ni NP chains with high magnification, the etched site is almost transparent meaning a quiet small amount of residues exist there. Fig. 6b gives the HR-TEM image of the etched site labeled by arrow in Fig. 5a, which shows the polycrystalline nature and the lattice fringes on the crystalline grain correspond to the plane (111) of CuO with FCC structure. This CuO polycrystalline structure was further verified by the SAED pattern in fig. 6c. Besides, a detailed characterization for Ni particle was also carried out, as shown in fig. 6d-6e. From fig. 6d we can see clearly the Ni segments show smooth boundary, the intuitive EDS characterization result shown in fig. S1. Fig. 6e shows a set of clear diffraction spots corresponding to Ni, where no spots for other impurities such as nickel oxide or nickel hydroxide were observed. The HR-TEM image (fig. 6f) proves that the lattice fringes in boundary are consistent with the lattice fringes in inside part, and all correspond to a face-centered cubic (FCC) structure of Ni. From the characterization results of Ni segment, we can judge the Ni segments are not affected throughout the corrosion process and are preserved completely.

### 3.4 Discussion for the corrosion mechanism

Since all of the experiment results shown in fig. 3 and fig. 5 are obtained after ultrasonic dispersion, in order to exclude the impact of ultrasound process on the formation of the NP chains, it is necessary to observe the corroded NWs arrays without ultrasonic dispersion which are shown in fig. 7a and fig. S2. It can be seen that the nanostructure also displays the NP chains morphology, which indicates the formation of NP chains has no relationship with the ultrasound process. Besides, we studied the morphology obtained with shorter corrosion time to explore the reaction process. Fig. 7b-d show the results of Ni/Cu NWs corroded with 15wt% NaOH solution for about 25min. From the FE-SEM image (fig. 7b) of the NWs dispersing on silicon wafer by ultrasonic, it can be seen that periodic breach appear on each NW, indicating that the corroding process has begun. The corresponding TEM result shown in fig. 7c gives more clear image, which reveals that most of the nanowires just be corroded slightly and exhibit a little tiny cracks, only the individual nanowires were etched to larger gaps. Fig. 7d shows the TEM image of single etched nanowire and the inset is the corresponding EDS element line scanning curve. It can be seen that although the periodic alternating of the two elements still can be observed in some sites, the periodically distributed Cu has been etched to some extent. The tiny cracks shown on the nanostructure of short corrosion time demonstrate the reaction product is soluble.

To the best of our knowledge, Cu is generally considered not to react with NaOH directly. Here, we deduce that the corroding of Cu in NaOH solution may be an electrochemical corrosion process, and NaOH solution is the electrolyte. This inference was further proved through a series of comparative experiments. Fig. 7e shows the characterization result when Ni/Cu NWs immersed in 3wt% NaCl saline solution for 1h. It can be seen that periodic blocks appear along the NWs. Fig. 7f shows the SEM image of Ni/Cu NWs immersed in deionized water for 3h, which have the similar morphology with fig.7e. Fig. 7g gives the corresponding TEM image of the structure in fig. 7e, which reveals the periodic blocks appear in the sites of Cu. It can be seen that the product was accumulated by multiple grain, and SAED (fig. 7h) and HR-TEM image (fig. 7i) corresponding to the grain label by arrow in fig. 7g indicate the blocky product is FCC CuO. As known, Cu could not react with NaCl or deionized water directly. Therefore, it can be concluded that the corrosion behaviour of Cu in NaCl solution and deionized water are both electrochemical corrosion, that is, Ni/Cu NW in neutral solution can form primary battery. By that analogy, we can deduce that the corrosion of Ni/Cu in NaOH solution is the electrochemical reaction, but different from the situation when electrolyte is neutral solution, the NaOH electrolyte would lead to the most of reaction products soluble.

The electrochemical reaction can be understood as follows. The electrochemical corrosion in neutral or alkaline solution is oxygen reduction reaction. A necessary condition for its occurrence is the electrode potential of the metal lower than the potential of oxygen reduction reaction. For Ni/Cu NW, Cu segments contact with Ni in both ends, as a result, there will be a

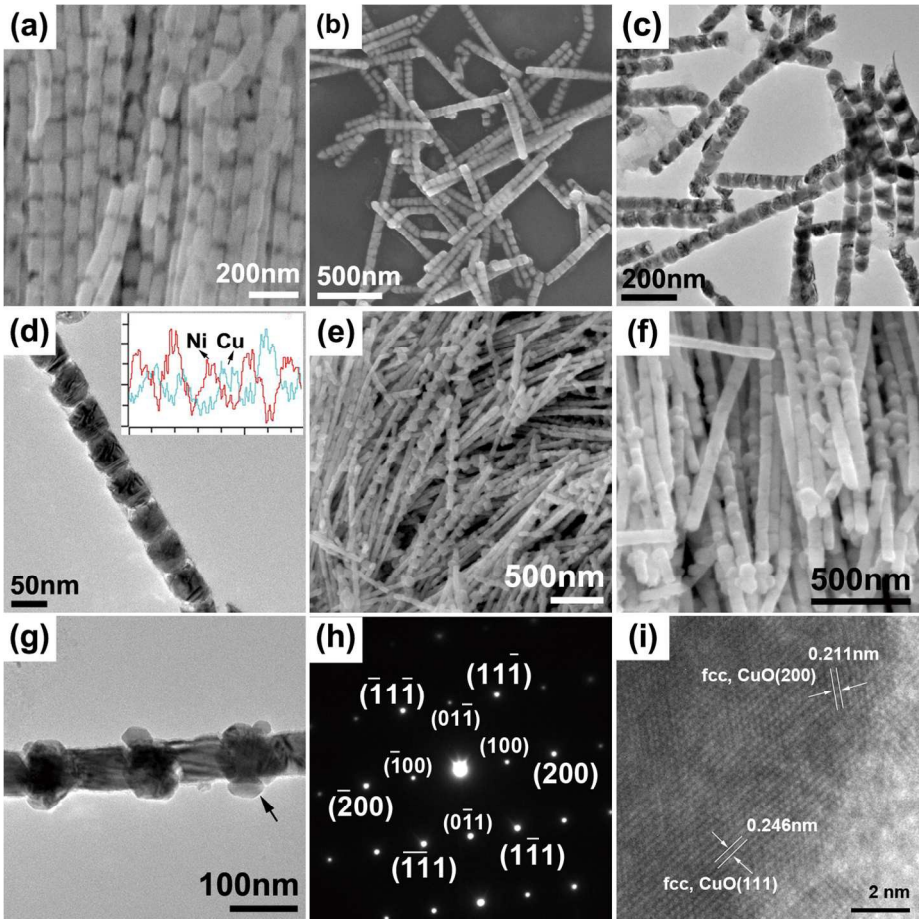


**Fig. 7** (a) SEM image of the NP chains arrays. SEM image (b) and TEM image (c) of nanowires etched in 15wt% NaOH solution for about 25min. (d) TEM image of single nanowires in (c) and the corresponding EDS element line scanning curve. FE-SEM images for Ni/Cu nanowires immersed in 3wt% NaCl saline solution for 1h (e) and in deionized water for 3h (f), and the corresponding TEM image for the corroded structure in NaCl solution (g), the SAED and HR-TEM image for the grin label by arrow in figure 6g (h-i).

number of contact primary batteries along the axial direction of Ni/Cu NW. In alkaline solution, the electrode potential of Cu (0.219V) is lower than the potential of oxygen reduction reaction (0.41V), while the electrode potential of Ni (0.72V) is higher than the potential of oxygen reduction reaction (see SI), therefore in each primary battery, Cu as the anode was corroded and Ni as the cathode was undamaged. Besides, it is believed that the electrochemical corrosion of Cu here is the galvanic corrosion (contact corrosion) resulting from the contact of two metals with different corrosion potential, which is because the experiment result demonstrates that the Cu segment as whole electrode involved the reaction and was removed entirely. If the electrochemical corrosion is just caused by the electrochemical heterogeneity present on the Cu surface, this means that some part of Cu acts as an electron source, which corresponds to the anode, and other part of Cu acts as an electron sink, which corresponds to the cathode, then Cu would present residues instead of all removed. As a contrast, we prepared pure copper nanowires arrays in AAO template and immersed them into 15 wt% NaOH solution for 50 min. The morphology of copper nanowires after corrosion (fig. 8) further validates this interpretation. Furthermore, it is also believed that oxygen existence is critical for the oxygen reduction reaction. Therefore, we performed the corrosion experiment for Ni/Cu NWs in 15wt% NaOH solution

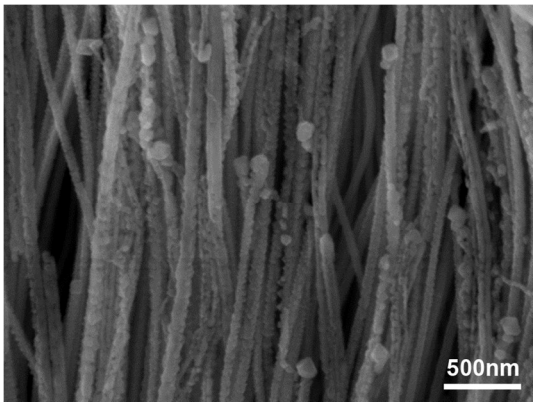


**Fig. 8** The morphology image of the Cu NWs arrays when corroded by 15wt% NaOH solution for 50 min.

under the approximate vacuum conditions, and at the same time the oxygen in solution has been removed (detailed operation see SI).The characterization results were shown in fig. 9. It is found that the Ni/Cu NWs have smooth surface and uniform diameter, and without slightest trace of etch. This result is the further evidence for the corrosion mechanism of oxygen reduction reaction.

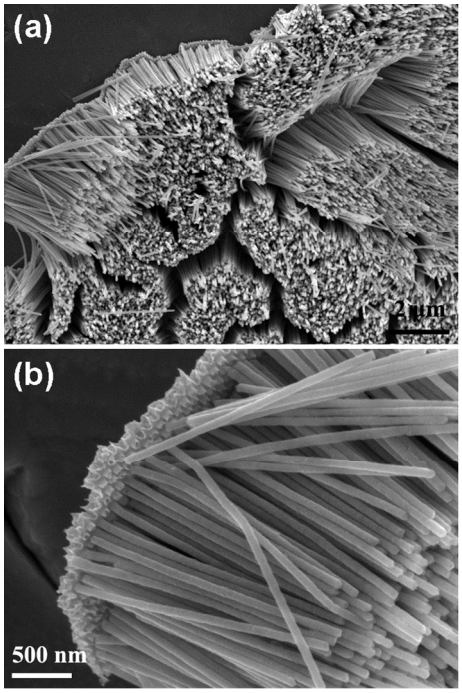


**Fig. 9** The morphology image of the Ni/Cu NWs arrays when corroded by 15wt% NaOH solution for 50min in oxygen-free environment.

As for the corrosion products generated in NaOH solution, some existed reports[40-45] may help us to facilitate understanding. It has been reported that the corrosion of Cu in the alkali solution is a complex process,[40-45] that is, solid production formed when the alkali solution is of low concentration, while the soluble production begin appear accompanying with the increase of the alkali solution concentration. Generally, the soluble product was thought to be Cu(II) which exists in the form of $HCuO^{2-}$, $Cu(OH)_4^{2-}$ or $CuO^{2-}$, and the solid product were $Cu_2O$, $Cu(OH)_2$ or CuO.[40,42,45] In addition, it has been reported that with the increase of the concentration of alkali solution, the proportion of soluble products wouldincreased.[40,41,43] In our experiment, the concentration of NaOH is 15 wt% which is a high value and the experiment result indicates that most of the products are soluble, which is consistent with the literature report.[40,41,43] The reaction that resulted in the soluble Cu(II) generation can be described by the following equations:[40, 43]

$$Cu + 3OH^- \rightarrow HCuO_2^- + H_2O + 2e \quad (1)$$

or

$$Cu + 4OH^- \rightarrow Cu(OH)_4^{2-} + 2e \quad (2)$$

or

$$Cu + 4OH^- \rightarrow CuO_2^{2-} + 2H_2O + 2e \quad (3)$$

It has been shown in Figure 6b that the solid product in the reaction is CuO, therefore the related reaction equation may be as follows:[44]

$$Cu + 2OH^- \rightarrow CuO + H_2O + 2e \quad (4)$$

The experiment result presented above can be understood clearly from this perspective. The scheme in Fig. 10 summarizes the development of Ni particle chains. When Ni/Cu segmented NW is surrounded by 15wt% NaOH solution (fig. 10a), electrons would transfer from Cu to Ni (fig. 10b) and an external circuit of the primary battery would be constituted as shown in fig. 10d. Cu as the anode is oxidized to Cu(II), and at the same time, oxygen in electrolyte solution gains electrons from the surface of Ni and the reduction reaction occurs. The reaction equation is:

$$O_2 + H_2O + 4e \rightarrow 4OH^- \quad (5)$$

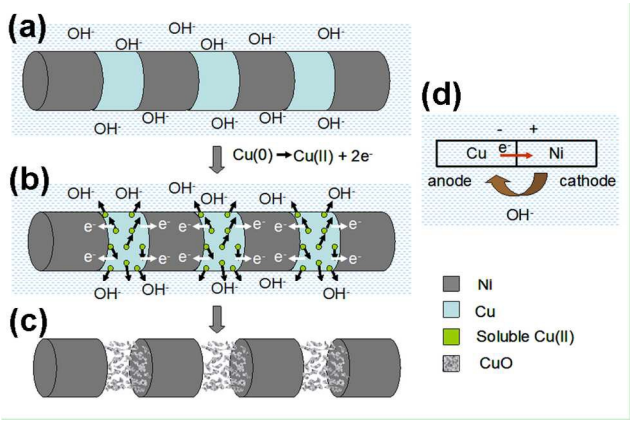


**Fig. 10** (a-c) Scheme for the formation process of Ni NP chains from Ni/Cu multi-segmented NWs. (d) Diagram for the primary battery circuit.

Hydroxyl in solution migrates from cathode Ni to anode Cu, forming the internal circuit of the primary battery (fig. 10d). Ni as the cathode only plays the role of electron transfer. Because the segments lengths of Ni and Cu are both dozens of nanometers, thus the $OH^-$ migration distance is very short, which leads to this reaction is fast. Among the anode product, the soluble Cu(II) move away from Cu segments (fig. 10b), leaving the small amount of solid CuO to link Ni segments (fig. 10c).

This electrochemical corrosion method is a facile and low-cost way for the NP chain nanostructures preparation. The particle size, separation and particle chain length can be adjusted easily. Given the fact that most metals can be fabricated by method of electrodeposition and the superlattice NWs containing two or more kinds of metals with different chemical activity can be prepared easily, therefore various kinds of metallic NP chain can be prepared by electrodeposition combined with the selective etching basing on the principle of primary batteries.

## 4 Conclusions

In summary, we have firstly fabricated Ni/Cu multi-segmented NWs via an alternate deposition method, and then successfully obtained Ni NP chains through etching Ni/Cu NWs in alkali solution. It is found that the Ni particle size and the spacing of the chains can be easily adjusted by controlling the length of Ni/Cu segments. The reaction mechanism is electrochemical corrosion, where Ni/Cu nanowire in the alkali environment form multiple primary batteries, in each battery, Ni as the cathode is remain unchanged, Cu as the anode is oxidized to Cu(II). The soluble Cu(II) move away from Cu segments, leaving the small amount of solid CuO films to link Ni segments. Our work shed light on extending the controllable fabrication of metallic NP chains nanostructures.

## Acknowledgement

This work was supported by National Basic Research Program of China (973 Program) (NO.2012CB932303), the National Natural Science Foundation of China (NOs.11204307, 51171176, 11404341), and the CAS/SAFEA International Partnership Program for Creative Research Teams.

## Notes and references

*Key Laboratory of Materials Physics, and Anhui Key Laboratory of Nanomaterials and Nanostructures, Institute of Solid State Physics, Hefei Institutes of Physical Science, Chinese Academy of Sciences, Hefei, 230031, P. R. China. Tel.: +86-551-65591453, Fax: +86-551-65591434, E-mail: gtfei@issp.ac.cn*

† Electronic Supplementary Information (ESI) available: EDS of Ni segment, morphology image ofNi NP chains arrays, electrode potential and operation process for approximate vacuum conditions.. See DOI: 10.1039/b000000x/

1 W. K. Hong, J. I. Sohn, D. K. Hwang, S. S. Kwon, G. Jo, S. Song, S. M. Kim, H. J. Ko, S. J. Park, M. E. Welland and T. Lee, *Nano Lett.,* 2008, **8**, 950-956.
2 Z. L. Xiao, C. Y. Han, W. K. Kwok, H. W. Wang, U. Welp, J. Wang and G. W. Crabtree, *J. Am. Chem. Soc.,* 2004, **126**, 2316-2317.
3 S. Wirth, S. von Molnár, M. Field, and D. D. Awschalom, *J. Appl. Phys.*, 1999, **85**, 5249-5254.
4 M. Quinten, A. Leitner, J. R. Krenn and F. R. Aussenegg, *Opt. Lett.*, 1998, **23**, 1331-1333.
5 S. A. Maier, M. L. Brongersma, P. G. Kik, S. Meltzer, A. A. G. Requicha and H. A. Atwater, *Adv. Mater.*, 2001, **13**, 1501-1505.
6 S. A. Maier,M. L. Brongersma, P. G. Kik and H. A. Atwater, *Phys. Rev. B*, 2002, **65**, 193408.
7 S. A. Maier, P. G. Kik, H. A. Atwater, S. Meltzer, E. Harel, B. E. Koel and A. A. G. Requicha, *Nat. Mater.,*2003, **2**, 229-232.
8 P. W. Chiu, G. Gu, G. T.Kim, G. Philipp, S. Roth, S. F. Yang and S. Yang, *Appl. Phys. Lett.,* 2001, **79**, 3845-3847.
9 H. Li, X. Q. Zhang, F. W. Sun, Y. F. Li, K. M. Liew and X. Q. He, *J. Appl. Phys.,* 2007, **102**, 013702.
10 C. H.Hsieh, L. J.Chou, G. R.Lin, Y.Bando and D. Golberg, *NanoLett.,*2008, **8**, 3081-3085.
11 M. S. Hu, H. L. Chen, C. H. Shen, L. S. Hong, B. R. Huang, K. H. Chen and L. C. Chen, *Nat. Mater.,* 2006, **5**, 102-106.
12 S. P. Li, D. Peyrade, M. Natali, A. Lebib and Y. Chen, *Phys. Rev. Lett.,* 2001, **86**, 1102-1105.
13 S. L. Tripp, R. E. Dunin-Borkowski and A. Wei, *Angew. Chem. Int. Ed.,* 2003, **42**, 5591-5593.
14 H. Wang, Y. Yu, Y. Sun and Q. Chen, *NANO: Brief Reports and Reviews,* 2011, **6**, 1-17.
15 C. Goubault, P. Jop, M. Fermigier, J. Baudry, E. Bertrand and J. Bibette, *Phys. Rev. Lett.,* 2003, **91**, 260802.
16 A. Koenig, P. Hebraud, C. Gosse, R. Dreyfus, J. Baudry, E. Bertrand and J. Bibette, *Phys. Rev. Lett.,* 2005, **95**, 128301.
17 X. W. Liu, Q. Y. Hu, Z. Fang, X. Gao, T. Jiang and P. F. Wei, *Journal of Crystal Growth,* 2010, **312**, 863-868.
18 V. Bliznyuk, S. Singamaneni, S. Sahoo, S. Polisetty, Xi. He and Ch. Binek, *Nanotechnology,* 2009, **20**, 105606.
19 T. Thurn-Albrecht, J. Schotter, C. A. Kastle, N. Emley, T. Shibauchi, L. Krusin-Elbaum, K. Guarini, C. T. Black, M. T. Tuominen and T. P. Russell, *Science,* 2000,**290**, 2126-2129.
20 C. A. Ross, *Annu. Rev. Mater. Res.,* 2001, **31**, 203-235.
21 Q. H. Wei, K. H. Su, S. Durant and X. Zhang, *Nano Lett.,* 2004, **4**, 1067-1071.
22 R. A. Mcmillan, C. D. Paavola, J. Howard, S. L. Chan, N. J. Zaluzec and J. D. Trent, *Nat. Mater.,* 2002, **1**, 247-252.
23 S. Kundu, K. Wang, H. Liang, *J. Phys. Chem. C,*2009, **113**, 134-141.
24 J. Fei, Y. Cui, A. Wang, P. Zhu and J. Li, *Chem. Commun.,* 2010, **46**, 2310-2312.
25 H. Jia, X. Tao, N. Li, L. Yu and L. Zheng, *CrytEngComm.,* 2011, **13**, 6179-6184.
26 M. E. Toimil-Molares, A. G. Balogh, T. W. Cornelius, R. Neumann and C. Trautmann, *Appl. Phys. Lett.,* 2004, **85**, 5337-5339.
27 S. Karim, M. E. Toimil-Morlares, A. G. Balogh, W. Ensinger, T. W. Cornelius, E. U. Khan and R. Neumann, *Nanotechnology,* 2006, **17**, 5954-5959.
28 Y. Qin, L. Liu, R. Yang,U. Gösele and M. Knez, *Nano Lett.,* 2008, **8**, 3221-3225.
29 Y. Qin, S. M. Lee, A. Pan, U. G. Gösele and M. Knez, *Nano Lett.,* 2008, **8**, 114-118.
30 J. A. Sioss and C. D. Keating, *NanoLett.,* 2005, **5**, 1779-1783.
31 L. D. Qin, S. Park, L. Huang and C. A. Mirkin, *Science,* 2005, **309**, 113-115.
32 S. H. Liu, J. B. H. Tok and Z. N.Bao, *NanoLett.,* 2005, **5**, 1071-1076.
33 L. Liu, W. Lee, R. Scholz, E. Pippel and U. Gösele, *Angew. Chem. Int. Ed.,* 2008, **47**, 7004-7008.
34 Y. Yang, L. Liu, F. Güder, A. Berger, R. Scholz, O. Albrecht and M. Zacharias, *Angew. Chem. Int. Ed.,* 2011, **50**, 10855-10858.
35 C. M. Liu, L. Guo, R. M. Wang, Y. Deng, H. B. Xu and S. Yang, *Chem. Comm.,* 2004, **23**, 2726-2727.
36 S. Singamaneni and V. Bliznyuk, *Appl. Phys. Lett.,* 2005, **87**, 162511.
37 Y. Yao, G. S. Chaubey and J. B.Wiley, *J. Am. Chem. Soc.,*2012, **134**, 2450-2452.
38 H. Masuda, H. Yamada, M Satoh, H. Asoh, M. Nakao and T. Tamamura, *Appl. Phys. Lett.,* 1997, **71**, 2770-2772.
39 S. H. Xu, G. T. Fei, X. G. Zhu, B. Wang, B. Wu and L. D. Zhang, *Nanotechnology,* 2011, **22**, 265602.
40 S. M. Abd EL Haleem and B. G. Ateya, *J. Electroanal. Chem.,* 1981, **117**, 309-319.
41 S. J. Dong, Y. W. Xie and G. J. Cheng, *Electrochimica Acta,* 1992, **37**, 17-22.
42 C-H. Pyun and S-M. Park, *J. Electrochem. Soc.: Electrochemical Science and Technology,* 1986, **133**, 2024-2030.
43 E. A. Ashour and B. G. Ateya, *Electrochimica Aata,* 1996, **42**, 243-250.
44 J. Ambrose, R. G. Barradas and D. W. Shoesmith, *Electroanalytical Chemistry and Interfacial Electrochemistry,* 1973, **47**, 47-64.
45 L. M. Abrantes, L. M. Castillo, C. Norman and L. M. Peter, *J. Electroanal. Chem.,* 1984, **163**, 209-221.

# The table of contents

Controllable Fabrication of Nickel Nanoparticle Chains Based on Electrochemical Corrosion

Shao Hui Xu, Guang Tao Fei*, Hao Miao Ouyang, Yao Zhang, Peng Cheng Huo and Li De Zhang

Ni nanoparticle chains are obtained by corroding Cu segments of Ni/Cu nanowires in alkali solution based on electrochemical corrosion.

ToC figure